

## Glueball properties in anisotropic SU(3) lattice QCD with improved action

Noriyoshi ISHII

*The Institute of Physical and Chemical Research(RIKEN),  
2-1 Hirosawa, Wako, Saitama 351-0198, JAPAN*

Hideo SUGANUMA

*Tokyo Institute of Technology,  
2-12-1 Ohkayama, Meguro, Tokyo 152-8552, JAPAN*

Hideo MATSUFURU

*Yukawa Institute for Theoretical Physics, Kyoto University,  
Kitashirakawa-Oiwake, Sakyo, Kyoto 606-8502, JAPAN*

We study the glueballs properties at finite temperature using  $SU(3)$  lattice QCD at the quenched level with the anisotropic lattice. We use the tree-level Symanzik  $O(a^2)$  improved action. We present our preliminary results which shows the slight reduction of the scalar glueball mass near  $T_c$ .

### 1 Introduction

The  $SU(3)$  lattice QCD Monte Carlo simulations suggest the existence of the finite temperature deconfinement transition at the critical temperature  $T_c \simeq 260$  MeV at the quenched level<sup>1</sup>. At the quenched level, without involving dynamical quark excitations, the lightest physical excitation is the scalar glueball with the mass  $1.5 \text{ GeV} \lesssim m_G \lesssim 1.7 \text{ GeV}$ <sup>2,3</sup>, which can be expected to dominate the thermodynamic properties below  $T_c$ . The closed packing model, a phenomenological model for the QCD phase transition, provides us with an intuitive picture that the deconfinement transition takes place when an “hadrons” excited from the thermal system begin overlap significantly with one another. However, since the contributions from the glueballs are suppressed by a rather strong statistical factor as  $e^{-m_G/T}$ , we may wonder if the total number of the glueballs to be excited may be insufficient in the quenched QCD. To keep the consistency with the closed packing model, the resolution may be found in either a tremendous expansion of the glueball size or a drastic reduction of the mass<sup>a</sup> near the critical temperature (See Fig.1). Indeed, the lattice result of the correlator of Polyakov loops supports the change in the shape of the  $q\bar{q}$  potential at finite temperature<sup>5,6</sup>. As a consequence, the phenomenological

---

<sup>a</sup>The reduction of a glueball mass is also anticipated in the monopole condensation picture of the confinement<sup>4</sup>.

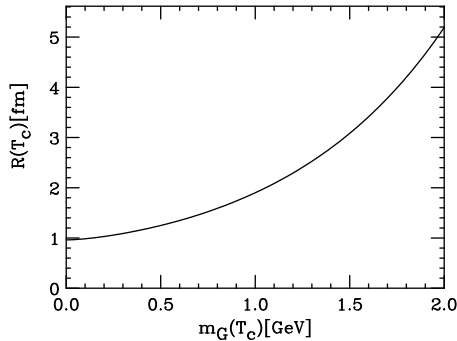


Figure 1: The glueball radius  $R(T_c)$  so as to reproduce  $T_c \simeq 260$  MeV in the closed packing model is plotted against the effective thermal glueball mass  $m_G(T_c)$ .

potential model suggests also the change in the wave function of the glueball particularly its mass and size. It is thus important to study the properties of glueballs at finite temperature, although no such studies have been done so far on the lattice. Even for typical hadrons, the most studies of the mass shift on the lattice at finite temperature are unfortunately limited to the screening mass, i.e., the correlation along the spatial direction<sup>7</sup>, whereas what is really interesting is the direct informations of the mass from the correlations along the temporal direction. This is because the lattice points available in the temporal direction decrease as the temperature becomes higher, and the extraction of the mass spectrum becomes more difficult. Recently, the use of the anisotropic lattice, where the temporal spacing is finer than the spatial one, has been established<sup>5,10</sup>, which enables us to overcome the difficulties mentioned above. In this paper, after analytical consideration with the closed packing model, we will outline how to study the glueball properties at finite temperature by means of the anisotropic lattice and the smearing method. We will present preliminary results in  $SU(3)$  lattice QCD with the tree-level Symanzik  $O(a^2)$  improved action.

## 2 The closed packing model for glueballs in the quenched QCD

In this section, we analytically investigate the deconfinement phase transition at the quenched level in terms of the low-lying scalar glueball properties. Consider the bag model picture of the scalar glueball. In this picture, a sphere of radius  $R$  distinguishes the outside from the inside, where the gluonic degrees of freedom appears. As long as the temperature  $T$  is low, the number  $N(T)$

of thermally excited bags is small. However, as the temperature increases, the number  $N(T)$  of bags increases. Finally, these bags begin to overlap each other and cover the whole space, and thus the deconfinement phase transition takes place in the closed packing model. The ratio of the volume inside the gluonic bags to the space volume  $V$  is given as

$$r_V(T) = \frac{\frac{4\pi}{3}R(T)^3 \times N(T)}{V} = \frac{4\pi}{3}R(T)^3 \int \frac{d^3k}{(2\pi)^3} \frac{1}{e^{E(\vec{k},T)/T} - 1}. \quad (1)$$

Now we simplify the dispersion relation to the quasi-free relation  $E(\vec{k}, T) = \sqrt{\vec{k}^2 + m_G^2(T)}$  with  $m_G(T)$  being the effective glueball mass at temperature  $T$ . Since the deconfinement phase transition is expected to take place when  $r_V(T) \simeq 1$ , the glueball radius  $R(T_c)$  near the deconfinement phase transition is estimated as

$$R(T_c) \simeq \left( \frac{4\pi}{3} \int \frac{d^3k}{(2\pi)^3} \frac{1}{e^{\sqrt{\vec{k}^2 + m_G^2(T_c)}/T_c} - 1} \right)^{-1/3}. \quad (2)$$

In Fig.1, the glueball radius  $R(T_c)$  so as to reproduce the deconfinement phase transition at  $T_c = 260$  MeV is plotted as the function of the glueball mass  $m_G(T_c)$  in the closed packing model. Thus, if  $m_G$  persists to be 1.7 GeV near  $T_c$ , the glueball should have the abnormally huge radius 3.8 fm. Instead, if  $R$  remains to be a typical hadron size about 1 fm, the glueball mass should reduce drastically as  $m_G(T_c) \lesssim 0.5$  GeV.

### 3 The smearing method in $SU(3)$ lattice QCD

Using  $SU(3)$  lattice QCD, we study the glueball correlator

$$G(t) \equiv \langle \tilde{O}(t)\tilde{O}(0) \rangle, \quad \tilde{O}(t) \equiv O(t) - \langle O \rangle, \quad O(t) \equiv \sum_{\vec{x}} O(t, \vec{x}). \quad (3)$$

The subtraction of the vacuum expectation value is necessary for the scalar glueball with  $J^{PC} = 0^{++}$ . The summation over  $\vec{x}$  physically means the momentum projection as  $\vec{p} = \vec{0}$ . In the case of the scalar glueball, the summand is<sup>2,3,11,12</sup>

$$O(t, \vec{x}) \equiv O_{12}(t, \vec{x}) + O_{23}(t, \vec{x}) + O_{31}(t, \vec{x}), \quad (4)$$

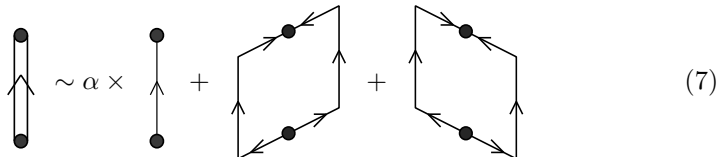
where  $O_{ij}(t, \vec{x})$  is the real part of the trace of the plaquette operator which lies within the  $i$ - $j$  plain. With the spectral representation,  $G(t)$  is expressed as as

$$G(t)/G(0) = \sum_{n=1}^{\infty} c_n e^{-E_n t}, \quad c_n \equiv \left| \langle n | \tilde{O} | 0 \rangle \right|^2 / G(0), \quad G(0) = \sum_{n=1}^{\infty} \left| \langle n | \tilde{O} | 0 \rangle \right|^2, \quad (5)$$

where  $E_n$  denotes the energy of the  $n$ -th excited state  $|n\rangle$ . (In this paper,  $|0\rangle$  denotes the vacuum, and  $|1\rangle$  denotes the ground-state  $0^{++}$  glueball.) Note that  $c_n$  is a positive number with  $\sum c_n = 1$ , and thus  $G(t)/G(0)$  can be expressed as a weighted average of the exponentials  $e^{-E_n t}$  with the weight  $c_n$ . On a finite lattice with the spacing  $a$ , the simple plaquette operator  $O_{ij}(t, \vec{x})$  has a small overlap with the glueball ground state  $|G\rangle \equiv |1\rangle$ , and the extracted mass from  $G(t)$  looks heavier owing to the excited-state contamination. This small overlap problem originates from that the plaquette operator has a smaller “size” of  $O(a)$  than the physical size of the glueball. This problem becomes severer near the continuum limit, i.e.,  $a \simeq 0$ . We thus have to enhance the overlap by improving the glueball operator so as to have approximately the same size as the physical size of the glueball. One of the systematic ways to achieve this is known to be the smearing method<sup>2,11,13,14</sup>. The smearing method is expressed as the iterative replacement of the original spatial link variables  $U_i(s)$  by the associated fat link variables,  $\bar{U}_i(s) \in SU(3)_c$ . The fat link variable  $\bar{U}_i(s)$  is defined to be the  $SU(3)_c$  element which maximizes

$$\text{ReTr} \left\{ \bar{U}_i^\dagger(s) \left[ \alpha U_i(s) + \sum_{j \neq i} \sum_{\pm} U_j(s) U_i(s \pm \hat{j}) U_j^\dagger(s \pm \hat{i}) \right] \right\}, \quad (6)$$

where  $U_{-\mu}(s) \equiv U_\mu^\dagger(s - \hat{\mu})$ , and  $\alpha$  is a real parameter. A schematic illustration of the fat link is given as



$$\text{fat link} \sim \alpha \times \text{link} + \text{loop}_1 + \text{loop}_2 \quad (7)$$

Note that the summation is only over the spatial direction to avoid the non-locality in the temporal direction. Note also that  $\bar{U}_i(s)$  holds the same gauge transformation properties with  $U_i(s)$ . We will refer to the fat link defined in Eq.(6) as the first fat link. The  $n$ -th fat link is defined iteratively, i.e., it is obtained by repeating the procedure in Eq.(6) with  $(n - 1)$ -th fat links. For the physically extended glueball operator, we use the  $n$ -th smeared operator, the plaquette operator which is constructed with the  $n$ -th fat link variables. To attribute a size to the  $n$ -th smeared operator, we use the linearization and the continuum approximation, and obtain the diffusion equation<sup>8</sup> as

$$\frac{\partial}{\partial n} \phi_i(n; \vec{x}) = D \Delta \phi_i(n; \vec{x}), \quad D \equiv \frac{a_s^2}{\alpha + 4}, \quad a_s : \text{spatial lattice spacing.} \quad (8)$$

Here  $\phi_i(n; \vec{x})$  denotes the distribution function of the gluon field  $A_i(\vec{x}, t)$  after the  $n$  smearing operations. The  $n$ -th smeared plaquette located at the origin  $\vec{x} = \vec{0}$  physically means the Gaussian extended glueball operator with the distribution as

$$\phi_i(n; \vec{x}) = \frac{1}{(4\pi Dn)^{3/2}} \exp\left[-\frac{\vec{x}^2}{4Dn}\right]. \quad (9)$$

Hence the size of the operator is estimated as

$$\sqrt{\langle \vec{x}^2 \rangle} = \sqrt{6Dn} = a_s \sqrt{\frac{6n}{\alpha + 4}}. \quad (10)$$

So far, the smearing method is introduced to carry out the accurate mass measurement by maximizing the overlap. However, it can be also used to give a rough estimate of the physical glueball size. In fact, once we obtain the maximum overlap with some  $n$  and  $\alpha$ , the physical size of the glueball is estimated with Eq.(10).

#### 4 The $SU(3)$ lattice QCD result for glueball mass and size at $T \neq 0$

In this section, we present our preliminary results. To generate the gauge field configurations, we use the tree-level Symanzik  $O(a^2)$  improved action<sup>9</sup>

$$S_G = \beta \frac{1}{\gamma_G} \sum_{s, i < j \leq 3} \left[ c_{11}(1 - P_{ij}(s)) + c_{12}(2 - R_{ij}(s) - R_{ji}(s)) \right] \\ + \beta \gamma_G \sum_{s, i \leq 3} \left[ c_{11}(1 - P_{i4}(s)) + c_{12}(2 - R_{i4}(s) - R_{4i}(s)) \right], \quad (11)$$

where  $c_{11} = 5/3$ ,  $c_{12} = -1/12$ ,  $\beta = 4.56$  and  $\gamma_G = 3.45$ .  $P_{\mu\nu}(s)$  is the plaquette and the rectangular loop  $R_{\mu\nu}(s)$  is defined as  $R_{\mu\nu}(s) = \frac{1}{3} \text{ReTr} \left( U_\mu(s) U_\mu(s + \hat{\mu}) U_\nu(s + 2\hat{\mu}) U_\nu^\dagger(s + \hat{\nu} + \hat{\mu}) U_\mu^\dagger(s + \hat{\nu}) U_\nu^\dagger(s) \right)$ . The numerical calculations are performed on the lattice of the sizes  $16^2 \times 24 \times N_t$ ,  $N_t = 28$  ( $T = 0.87T_c$ ) and  $N_t = 96$  ( $T \simeq 0$ )<sup>5,10</sup>. These parameters generate the spatial lattice spacing as  $a_s = 0.12$  fm and the temporal lattice spacing as  $a_t = 0.03$  fm. We have used 500 gauge field configurations for  $N_t = 28$  and 150 for  $N_t = 96$ . Throughout this section, we take the smearing parameter as  $\alpha = 2.3$ .

In Fig.2, the the overlap  $C \equiv \left| \langle G | \tilde{O} | 0 \rangle \right|^2 / G(0)$  and  $\chi^2 / N_{\text{DF}}$  are plotted against the iteration number of the smearing  $N_{\text{smear}} (= n)$ . The overlap becomes maximum with reasonable  $\chi^2$  as  $\chi^2 / N_{\text{DF}} \lesssim 1$  in the region  $10 \leq N_{\text{smear}} \leq 24$ . In this region, as is shown in Fig.3, the glueball mass, which is

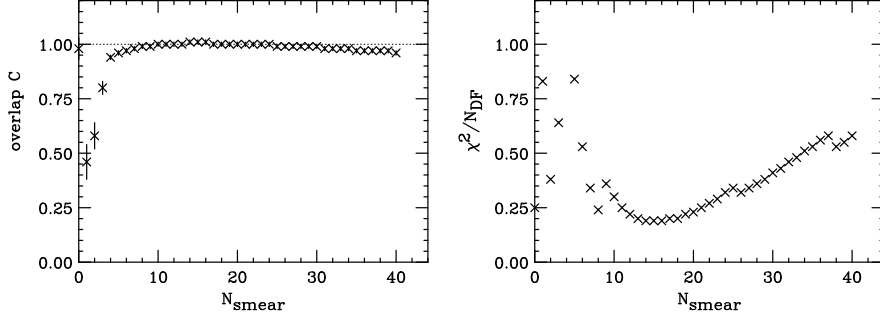


Figure 2: The overlap  $C$  is plotted against  $N_{\text{smear}}$  at  $T = 0$  (left figure).  $\chi^2/N_{\text{DF}}$  is plotted against  $N_{\text{smear}}$  at  $T = 0$  (right figure).

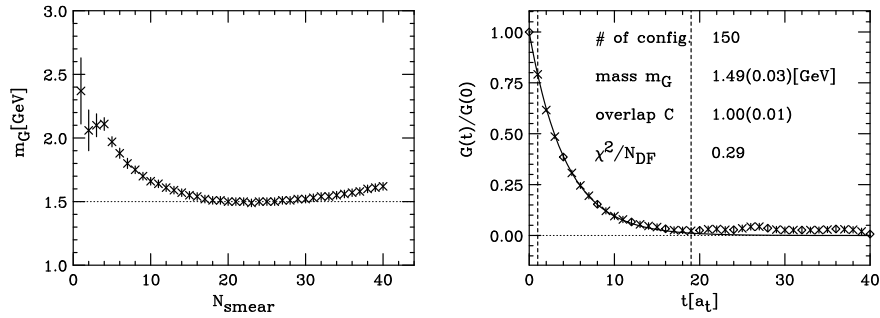


Figure 3: The glueball mass  $m_G$  is plotted against  $N_{\text{smear}}$  (left figure). The normalized glueball correlator  $G(t)/G(0)$  at  $T = 0$  is plotted at  $N_{\text{smear}} = 23$  (right figure). The curve denotes the best single-exponential fit from the region between the vertical dotted lines.

extracted with the single-exponential fit, takes its minimum as  $m_G = 1.49$  GeV at  $N_{\text{smear}} = 23$ . This indicates the achievement of the ground-state glueball. We thus obtain  $m_G = 1.49$  GeV at  $T = 0$ . The glueball size  $R$  is estimated with Eq.(10) as  $0.37 \text{ fm} \lesssim R \lesssim 0.57 \text{ fm}$  from the maximal overlap region as  $10 \leq N_{\text{smear}} \leq 24$ . We show also the glueball correlator  $G(t)$  at  $T = 0$  for a smearing number  $N_{\text{smear}} = 23$  in Fig.3. Note that, if we used the isotropic lattice, we could only use the points indicated by the diamond symbols, which would be inefficient to get the mass.

At finite temperature, we use the hyperbolic cosine fitting as  $G(t)/G(0) = C(e^{-m_G t a_t} + e^{-m_G(N_t - t)a_t})$ , where  $N_t$  denotes the number of the temporal lattice size, and  $a_t$  the temporal lattice spacing. In Fig.4, the overlap  $C$  and  $\chi^2/N_{\text{DF}}$  for  $T = 0.87T_c$  are plotted against  $N_{\text{smear}}$ . In the whole region, we

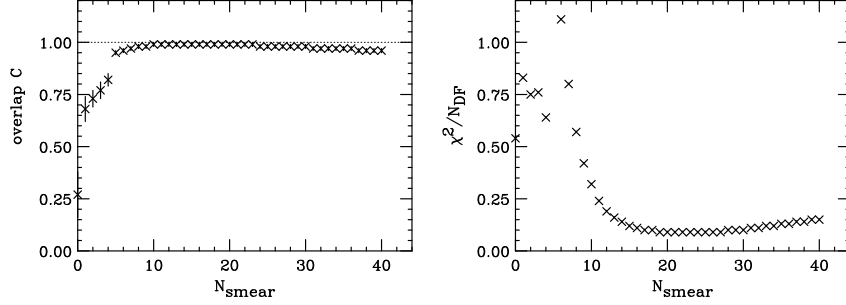


Figure 4: The overlap  $C$  is plotted against  $N_{\text{smear}}$  at  $T = 0.87T_c$  (left figure).  $\chi^2/N_{\text{DF}}$  is plotted against  $N_{\text{smear}}$  at  $T = 0.87T_c$  (right figure).

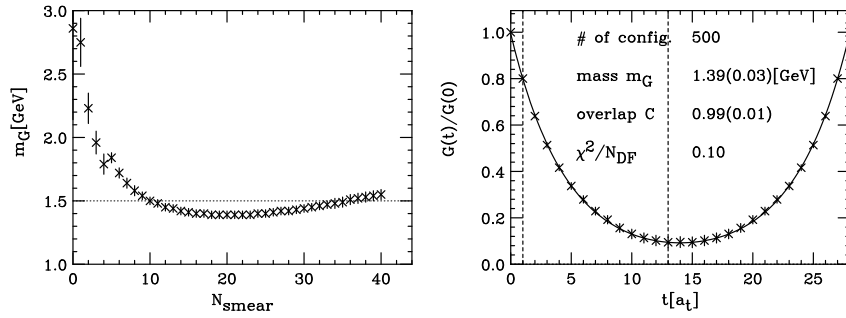


Figure 5: The fitted glueball mass at  $T = 0.87T_c$  is plotted against  $N_{\text{smear}}$  (left figure). The normalized glueball correlator  $G(t)/G(0)$  at  $T = 0.87T_c$  is plotted for  $N_{\text{smear}} = 23$  (right figure). The curve denotes the best hyperbolic cosine fit with the interval indicated by the vertical dotted lines.

have reasonable  $\chi^2$  as  $\chi^2/N_{\text{DF}} \lesssim 1$ . The overlap becomes maximum in the region  $10 \leq N_{\text{smear}} \leq 23$ . In this region as is shown in Fig.5, the glueball mass becomes minimum as  $m_G = 1.39$  GeV in the interval  $18 \leq N_{\text{smear}} \leq 23$ . We thus obtain  $m_G = 1.39$  GeV at  $T = 0.87T_c$ . The glueball size  $R$  is also estimated with Eq.(10) as  $0.37 \text{ fm} \lesssim R \lesssim 0.56 \text{ fm}$  at  $T = 0.87T_c$  from the maximal overlap region as  $10 \leq N_{\text{smear}} \leq 23$ . We show also the glueball correlator  $G(t)$  at  $T = 0.87T_c$  for  $N_{\text{smear}} = 23$  in Fig.5.

## 5 Summary and discussions

We have applied the closed packing model to the quenched QCD to derive the relation between the mass and the size of the glueball so as to reproduce

the deconfinement phase transition at  $T_c = 260$  MeV. We have then studied the mass and the size of the scalar glueball at finite temperature by using  $SU(3)$  lattice QCD at the quenched level with the anisotropic lattice and the smearing method. To generate the gauge field configurations, we have used the tree-level Symanzik  $O(a^2)$  improved action with the lattice size  $16^2 \times 24 \times N_t$ ,  $N_t = 96(T = 0)$  and  $N_t = 28(T = 0.87T_c)$ . As for the glueball size  $R(T)$ , no drastic change has been observed between  $0.37 \text{ fm} \lesssim R(T = 0) \lesssim 0.57 \text{ fm}$  and  $0.37 \text{ fm} \lesssim R(T = 0.87T_c) \lesssim 0.56 \text{ fm}$ . We have obtained the glueball mass  $m_G = 1.49 \text{ GeV}$  at  $T = 0$  and  $m_G = 1.39 \text{ GeV}$  at  $T = 0.87T_c$ . This result may suggest the slight reduction of the glueball mass at finite temperature, which would provide a support for our conjecture discussed in Sect. 1 and Sect. 2. However, this reduction does not seem so drastic as is suggested by the closed packing model for the quenched QCD. At any rate, to draw a definite conclusion, much more statistics are necessary.

### Acknowledgements

The calculations have been performed on the NEC SX-5 in Osaka University. The authors thank Dr. T. Umeda for useful comments and discussions.

### References

1. G. Boyd, J. Engels, F. Karsch, E. Laermann, C. Legeland, M. Lutgemeier and B. Petersson, *Nucl. Phys. B* **469**, 419 (1996).
2. C. Moningstar and M. J. Peardon, *Phys. Rev. D* **60**, 034509 (1999).
3. J. Sexton, A. Vaccarino, D. Weingarten, *Phys. Rev. Lett.* **75**, 4563 (1995).
4. H. Ichie, H. Suganuma and H. Toki, *Phys. Rev. D* **52**, 2944 (1995).
5. H. Matsufuru, Y. Nemoto, H. Suganuma, T. T. Takahashi and T. Umeda, Proceedings of *Quantum Chromodynamics and Color Confinement*, edited by H. Suganuma et al. (World Scientific, 2001) 246.
6. O. Kaczmarek, F. Karsch, E. Laermann and M. Lutgemeier, *Phys. Rev. D* **62**, 034021 (2000).
7. C. DeTar and J. B. Kogut, *Phys. Rev. Lett.* **59**, 399 (1987).
8. N. Ishii, H. Suganuma and H. Matsufuru, in preparation.
9. K. Symanzik, *Nucl. Phys. B* **226**, 187 (1983).
10. T. R. Klassen, *Nucl. Phys. B* **533**, 557 (1998).
11. H. J. Rothe, *Lattice Gauge Theories*, (World Scientific, 1992) 1.
12. I. Montvay and G. Münster, *Quantum Fields on a Lattice*, (Cambridge Monographs on Mathematical Physics, 1994) 1.
13. APE Collaboration, M. Albanese et al., *Phys. Lett. B* **192**, 163 (1987).
14. T. T. Takahashi, H. Matsufuru, Y. Nemoto and H. Suganuma, *Phys. Rev. Lett.* **86**, 18 (2001).